Solution of the Finite Length Septum Problem with Application to Periodic Mode Suppressors

SIDNEY B. FRANKLIN, MEMBER, IEEE

Abstract—**A square waveguide with periodic septums is considered with a view towards determining the parameters of a structure which suppresses three of four possible propagating modes. The analysis is presented in two parts, the first of which is concerned with the isolated septum. Using available techniques, semi-infinite scattering matrices are determined for the semi-infinite septum for arbitrary TE_{N0}, TE_{N1}, and TM_{N1} incident modes. These are used to derive Fredholm matrix equations which yield the field everywhere near the finite length septum. The leading terms of the inverted equations are the far-field transmission and reflection coefficients. The solutions are evaluated for several frequencies, and fifth degree polynomials are fitted for the computation of S_{11} and S_{12}. The analysis for the TE_{10} mode is applicable to an arbitrary height waveguide and may be used without modification for the "finite length" septum in conventional waveguide.**

The second part is concerned with the periodic waveguide and assumes that the septums are far apart. A contour chart is introduced to visualize the performance of the periodic structure. The chart is especially useful when more than one propagating mode is involved and simplifies the design problem so that the parameters of practical structures may be obtained with little effort.

Introduction

IN RECENT YEARS there has been a considerable effort [1]–[4] to develop waveguides for use in the higher microwave frequency range, which are capable of transmitting large amounts of power with low attenuation. Since power capacity is proportional to cross-sectional area, this usually leads to large waveguides with multimode capability, or to open waveguides. For many applications, such as airborne radar, open structures are not feasible. Conversely, oversize waveguides inevitably have imperfections which induce unwanted modes.

Paralleling waveguides can increase power capacity, but with no reduction in attenuation. If the parallel waveguides are arranged to have common walls, with opposite current flow on each side, I^2R losses may be reduced by eliminating the common wall. For two rectangular waveguides in parallel, the result is a square waveguide; many such rectangular waveguides in parallel produce a tall waveguide. Completely eliminating the common walls creates structures which are again capable of multimode propagation. Thus partial elimination is called for, leading to a structure with septums at periodic intervals.

The attenuation of a rectangular waveguide is 45 to 61 percent greater than that of a square waveguide with no septums. Thus, for certain applications, square waveguide with short, widely spaced septums may be justified, and will be considered here.

Rectangular waveguides are normally operated in the TE_{10} mode between 1.24 and $1.87 f_{co}$. When the guide is enlarged to a square shape, three additional modes are possible: the TE_{01} mode over the same band as the TE_{10} mode, and the TE_{11} and TM_{11} modes whose cutoff frequency is 1.414 that of the TE_{10} mode. Here it is assumed that the TE_{01} mode is the desired propagating mode and that the TE_{10}, TE_{11}, and TM_{11} modes are to be rejected. This permits the analysis for the TE_{10} mode to apply directly to the H-plane finite-length septum problem in conventional rectangular waveguide.

Thin septums in the y–z plane are transparent to the TE_{01} mode and no further analysis for this mode is required. The reduction of attenuation is equal to the difference in attenuation of square and rectangular waveguide times the factor, $D/L' = 1-(L/L')$, where D is the distance between septums, L is the septum length, and L' is the period of the structure.

The design engineer's main concern is to choose the shortest possible septum length and the largest spacings which, at the same time, have a maximum inhibiting effect on the undesired modes. The analysis for these modes can be reduced to determining the scattering parameters of isolated septums for subsequent determination of the stopbands of the periodic structure.

The Scattering Matrix Approach

Consider a geometrically symmetrical $2N$-port with even or odd excitation. The field scattered from one port is the same as if the structure is bisected with a magnetic or electric wall, and excited from one side only. It has been shown [5] that the scattering matrix of the $2N$-port is reducible to combinations of the reflection matrices obtained from the bisected structure. Let $\bar{a}$ be an N-vector representing the amplitude of the modes incident on the bisected structure, $\bar{b}$ an N-vector representing the amplitude of the reflected modes. Then:

$$\bar{b} = \Gamma_{e,o}\bar{a} \tag{1}$$

where $\Gamma_{e,o}$ is the reflection matrix and the subscripts indicate even or odd excitation (magnetic or electric walls for TE modes).

For the symmetric $2N$-port of Fig. 1

$$\begin{bmatrix} \overline{b_1} \\ \overline{b_2} \end{bmatrix} = \begin{bmatrix} \overline{S_{11}} & \overline{S_{12}} \\ \overline{S_{22}} & \overline{S_{22}} \end{bmatrix} \begin{bmatrix} \overline{a_1} \\ \overline{a_2} \end{bmatrix}$$

Manuscript received June 10, 1966; revised December 21, 1966. The material in this paper is based upon a dissertation submitted in partial fulfillment of the requirements for the doctoral degree at the University of Illinois, Urbana, Ill.

The author is in the U. S. Air Force, Military Research and Development Center, OSD/ARPA R&D Field Unit, Bangkok, Thailand.

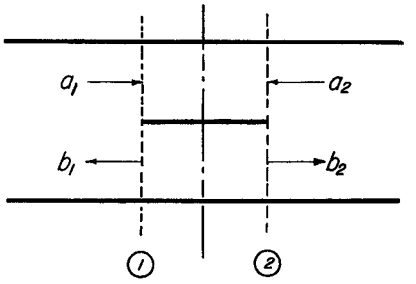

Fig. 1. A symmetric $2N$-port.

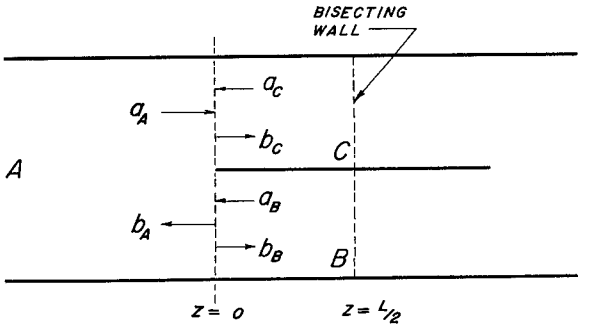

Fig. 2. The bisected structure, with a magnetic or an electric wall.

where

$$\overline{S_{11}} = \overline{S_{22}} = \tfrac{1}{2}(\Gamma e + \Gamma o)$$

$$\overline{S_{12}} = \overline{S_{21}} = \tfrac{1}{2}(\Gamma e - \Gamma o).$$

In three excellent reports, Pace and Mittra [6]–[8] introduced the Generalized Scattering Matrix which includes the evanescent modes as well as the propagating modes. Assuming generalized scattering matrices, (1) becomes an infinite set of equations, where the first N-components of $\bar{a}$ and $\bar{b}$ are the amplitudes of the propagating modes and the remaining terms represent the amplitude of the evanescent modes.

It follows from (2) that for $N=1$, the far-field reflection and transmission coefficients, (Γ and τ) are $\frac{1}{2}(\Gamma e_{11}+\Gamma o_{11})$ and $\frac{1}{2}(\Gamma e_{11}-\Gamma o_{11})$, respectively. Thus, by considering the problem of the bisected structure, it is possible to determine the fields everywhere, as well as Γ and τ.

The Bisected Structure

Consider the bisected septum of Fig. 2, with $z=0$ located at the leading edge of the septum. The vectors $\bar{a}$ and $\bar{b}$ are related by the partitioned matrix:

$$\begin{bmatrix} \bar{b}_A \\ \bar{b}_B \\ \bar{b}_C \end{bmatrix} = \begin{bmatrix} S_{AA} & S_{AB} & S_{AC} \\ S_{BA} & S_{BB} & S_{BC} \\ S_{CA} & S_{CB} & S_{CC} \end{bmatrix} \begin{bmatrix} \bar{a}_A \\ \bar{a}_B \\ \bar{a}_C \end{bmatrix}. \tag{3}$$

The elements of the submatrices, $S_{\mu\nu}$, are obtained by considering the semi-infinite septum problem, and will be discussed in a later section.

From Fig. 2

$$\bar{a}_B = r_o^e T_B b_B$$

$$\bar{a}_C = r_o^e T_C \bar{b}_C \tag{4}$$

where

$$T_B = \begin{bmatrix} e^{-\gamma_{B_1} L} & & & 0 \\ & e^{-\gamma_{B_2} L} & & \\ & & e^{-\gamma_{B_3} L} & \\ 0 & & & \ddots \end{bmatrix} \tag{5}$$

and $r_e=+1$, $r_o=-1$. T_C is similar to T_B, and is equal to it when the septum is centered. Then (3) becomes:

$$\begin{bmatrix} \bar{b}_A \\ \bar{b}_B \\ \bar{b}_C \end{bmatrix} = \begin{bmatrix} S_{AA} & S_{AB} & S_{AC} \\ S_{BA} & S_{BB} & S_{BC} \\ S_{CA} & S_{CB} & S_{CC} \end{bmatrix} \begin{bmatrix} \bar{a}_A \\ r\ T_B\ \bar{b}_B \\ r\ T_C\ \bar{b}_C \end{bmatrix}. \tag{6}$$

The present analysis will restrict the problem to centered septums and to incident modes affected by the septum. The latter condition permits $\bar{a}_A$ and $\bar{b}_A$ to be restricted to modes having transverse E-fields which are symmetrical in x about the septum. With this restriction, $\gamma_{B_i}=\gamma_{C_i}=\beta_i$; $T_B=T_C=T$ and $\bar{b}_B$ and $\bar{b}_C$ are related by $\bar{b}_B=II\bar{b}_C$, where II is a diagonal matrix. II is the identity matrix, or the identity matrix with the even diagonal terms negative, depending on the choice of the $x=0$ position. In either event, $II^{-1}=II$. With this understanding, the second equation of (6) becomes:

$$\bar{b}_B = S_{BA}\bar{a}_A + r(S_{BB} + S_{BC}II)T\bar{b}_B \tag{7}$$

where use has been made of the fact that both T and II are diagonal and commute. This is a Fredholm matrix equation, and can be solved for $\bar{b}_B$ if none of its eigenvalues are equal to one. This was shown to be true by Pace and Mittra. Then

$$\bar{b}_B = [I - r(S_{BB} + S_{BC}II)T]^{-1}S_{BA}\bar{a}_A \tag{8}$$

and

$$\bar{b}_A = S_{AA}\bar{a}_A + r(S_{AB} + S_{AC}II)T[I - r(S_{BB} + S_{BC}II)T]^{-1}S_{BA}\bar{a}_A. \tag{9}$$

The Unbisected Structure

If $\bar{a}_A$ is replaced by I, it is necessary to replace $\bar{b}_A$ by Γ_e or Γ_o, depending on r_e or r_o. Combining this with (8) and (9), the results for the complete septum without the bisecting wall are:

$$\overline{S_{11}} = S_{AA} + \tfrac{1}{2}(S_{AB} + S_{AC}II)T \cdot \begin{Bmatrix} [I - (S_{BB} + S_{BC}II)T]^{-1} \\ -[I + (S_{BB} + S_{BC}II)T]^{-1} \end{Bmatrix} S_{BA} \tag{10a}$$

$$\overline{S_{12}} = \tfrac{1}{2}(S_{AB} + S_{AC}II)T \cdot \begin{Bmatrix} [I - (S_{BB} + S_{BC}II)T]^{-1} \\ +[I + (S_{BB} + S_{BC}II)T]^{-1} \end{Bmatrix} S_{BA}. \tag{10b}$$

The field in the septum region is the sum of the fields obtained from the solution of the even and odd excitation problem, or from (8)

$$\bar{b}_B\Big|_{\substack{\text{unbisected}\\ \text{septum}}} = \tfrac{1}{2}\{[I - (S_{BB} + S_{BC}II)T]^{-1} + [I + (S_{BB} + S_{BC}II)T]^{-1}\}S_{BA}\bar{a}_A \quad (11a)$$

$$\bar{a}_B\Big|_{\substack{\text{unbisected}\\ \text{septum}}} = \tfrac{1}{2}T\{[I - (S_{BB} + S_{BC}II)T]^{-1} - [I + (S_{BB} + S_{BC}II)T]^{-1}\}S_{BA}\bar{a}_A. \quad (11b)$$

The Matrix Elements

Let the vectors $\bar{a}_A$, $\bar{a}_B$, or $\bar{a}_C$ be restricted so that two are null vectors and the third $\bar{a}_\nu$ is the unit vector corresponding to zero for all but the Jth element, which is 1.0. From (3), the vectors $\bar{b}_A$, $\bar{b}_B$, and $\bar{b}_C$ are each column vectors of the submatrices $S_{A\nu}$, $S_{B\nu}$, and $S_{C\nu}$. Then, to obtain the matrix elements, it is only necessary to assume a single mode incident on the edge of the semi-infinite septum from one of the three regions. The amplitudes of the modes scattered in the three regions become the elements of one column of three of the submatrices of (3). The remaining six matrices are determined by changing ν from A to B to C.

a) *The TE_{N0} Fields and Matrix Elements:* This problem has been discussed by Hurd and Gruenberg [9] for the TE_{N0} modes only, assuming the simultaneous incidence of the lowest-order mode in each of the three regions, and a septum location such that b/a is irrational. It is a relatively simple matter to generalize their results for any incident mode, and to allow for the degeneracy which results when $b/a=\frac{1}{2}$.

Let the transverse E-fields be expanded in a Fourier series with respect to Fig. 3 and the following modal coordinate sets:

$$\left\{\phi_{A_{hn}} = \mathcal{Y}\sin\left((2n-1)\frac{\pi x}{a}\right)\right\}_n$$

$$\left\{\phi_{B_{hn}} = \mathcal{Y}\sin\frac{n\pi x}{b}\right\}_n$$

$$\left\{\phi_{C_{hn}} = \mathcal{Y}\sin\frac{n\pi(x-b)}{b}\right\}_n. \quad (12)$$

Then the incident and reflected transverse E-fields in Region A are

$$E_{\text{incident }A} = \sum_{n=1}^{\infty} a_{A_n}\phi_{A_{hn}}e^{-\gamma_{A_{hn}}z} \quad (13a)$$

$$E_{\text{reflected }A} = \sum_{n=1}^{\infty} b_{A_n}\phi_{A_{hn}}e^{+\gamma_{A_{hn}}z} \quad (13b)$$

where

$$\gamma_{A_{hn}} = \alpha_n = \left[\left((2n-1)\frac{\pi}{a}\right)^2 - k_0^2\right]^{1/2}. \quad (14a)$$

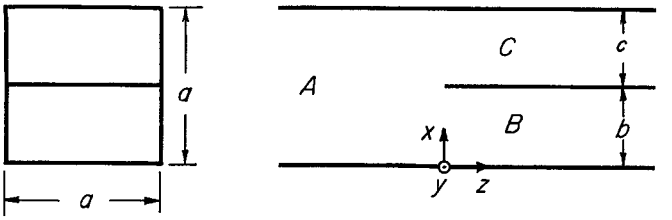

Fig. 3. The semi-infinite septum.

There are similar equations for regions B and C, providing

$$\gamma_{B_{hn}} = \gamma_{C_{hn}} = \beta_n = \left[\left(\frac{n\pi}{b}\right)^2 - k_0^2\right]^{1/2}. \quad (14b)$$

Note that the coefficients from (13a) and (13b) are the elements of the semi-infinite vectors $\bar{a}_A$ and $\bar{b}_A$. For this choice of geometric coordinate system, the matrix II becomes

$$II_{IJ} = (-1)^{J+1}\delta_{IJ}.$$

The elements of the matrices of (10) are:

$$S_{AAIJ} = (-1)^{I+J}\frac{r_h(\alpha_I, -\alpha_J)}{r_h(-\alpha_J, -\alpha_J)}F_1$$

$$\tfrac{1}{2}(S_{AB} + S_{AC}II)_{IJ} = (-1)^{I+J}\frac{\beta_J b^2 r_h(\alpha_I, \beta_J)}{\pi J h(\beta_J, \beta_J)}F_2$$

$$(S_{BB} + S_{BC}II)_{IJ} = (-1)^{I+J+1}\frac{I\beta_J h(-\beta_I, \beta_J)}{J\beta_I h(\beta_J, \beta_J)}F_3$$

$$S_{BAIJ} = (-1)^{I+J+1}\frac{\pi I h(-\beta_I, -\alpha_J)}{\beta_I b^2 r_h(-\alpha_J, -\alpha_J)}F_4 \quad (15)$$

where:

1) $h(\xi, \eta) = \dfrac{\pi(\xi, \beta_n)}{(\xi - \eta)\pi(\xi, \alpha_n)}\exp\left[-\dfrac{a}{\pi}\xi\ln\dfrac{b}{a}\right]$ (16)

2) $r_h(\xi, \eta)$ is the residue of $h(\xi, \eta)$ at the pole ξ

3) $\pi(\xi, \beta_n) = \prod_{n=1}^{\infty}(\beta_n - \xi)\dfrac{b}{n\pi}\exp\left[\dfrac{b\xi}{n\pi}\right]$ (17)

4) $\pi(\xi, \alpha_n) = \prod_{n=1}^{\infty}(\alpha_n - \xi)\dfrac{a}{(2n-1)\pi}\cdot \exp\left[\dfrac{a\xi}{(2n-1)\pi}\right]$. (18)

5) F_1, F_2, F_3, and F_4 are factors which will be used to relate the TE problem to the TM problem. Here they are equal to one.

b) *The TE_{N1} Problem:* The TE_{N1} solution is formally identical to the TE_{N0} solution if the modal coordinates are chosen as follows:

$$\left\{\phi_{A_{hn}} = -\frac{1}{2n-1}\cos\frac{(2n-1)\pi x}{a}\sin\frac{\pi y}{a}\hat{x} + \sin\frac{(2n-1)\pi x}{a}\cos\frac{\pi y}{a}\hat{y}\right\}_n$$

$$\left\{\phi_{B_{hn}} = -\frac{1}{2n}\cos\frac{n\pi x}{b}\sin\frac{\pi y}{a}\hat{x} + \sin\frac{n\pi x}{b}\cos\frac{\pi y}{a}\hat{y}\right\}_n$$

$$\left\{\phi_{C_{hn}} = -\frac{1}{2n}\cos\frac{n\pi(x-b)}{b}\sin\frac{\pi y}{a}\hat{x} + \sin\frac{n\pi(x-b)}{b}\cos\frac{\pi y}{a}\hat{y}\right\}_n \quad (19)$$

and if k_0^2 in α_n and β_n is replaced by $k_0^2-(\pi/a)^2$.

c) *The TM_{N1} Fields and Matrix Elements:* The approach of Hurd and Gruenberg may also be used for the field analysis of the TM_{N1} mode problem, but it is not quite as straightforward because the transverse fields have two components instead of one as in the TE_{NO} problem. The main effect of the additional field component is in the determination of two constants in their "function-theoretic" approach. For the TE_{N0} problem, the "edge condition" [10] allows one constant to be zero. For the TM_{N1} problem, this is not the case and a series expansion for E_y can be shown to be uniformly convergent in the aperture and at the end points. This expansion converges to E_y at all points in the aperture and must also converge to E_y at the end points. Thus, the additional equation is obtained by equating this expansion to zero at the septum edge.

Let the transverse H-fields be expanded in a Fourier series with respect to the following modal coordinate sets:

$$\left\{\phi_{A_{en}} = \frac{1}{\sqrt{1+(2n-1)^2}}\left[-\sin\left((2n-1)\frac{\pi x}{a}\right)\cos\frac{\pi y}{a}\hat{x} + (2n-1)\cos\left((2n-1)\frac{\pi x}{a}\right)\sin\frac{\pi y}{a}\hat{y}\right]\right\}_n$$

$$\left\{\phi_{B_{en}} = \frac{1}{\sqrt{1+4n^2}}\left[-\sin\frac{n\pi x}{b}\cos\frac{\pi y}{a}\hat{x} + 2n\cos\frac{n\pi x}{b}\sin\frac{\pi y}{a}\hat{y}\right]\right\}_n$$

$$\left\{\phi_{C_{en}} = \frac{1}{\sqrt{1+4n^2}}\left[-\sin\frac{n\pi(x-b)}{b}\cos\frac{\pi y}{a}\hat{x} + 2n\cos\frac{n\pi(x-b)}{b}\sin\frac{\pi y}{a}\hat{y}\right]\right\}_n . \quad (20)$$

In (13a) and (13b) replace E by H and in (14) replace k_0^2 by $k_0^2-(\pi/a)^2$. Then the vectors $\bar{a}$ and $\bar{b}$ represent the amplitude of the transverse H-modes instead of the transverse E-modes. The elements of the matrices of (10) are given by (15) and the factors F_i take the following form:

$$F_1 = \sqrt{\frac{1+(2J-1)^2}{1+(2I-1)^2}}\,\frac{1+\alpha_I\frac{\epsilon_1}{\epsilon_0}(-\alpha_J)}{1-\alpha_J\frac{\epsilon_1}{\epsilon_0}(-\alpha_J)}$$

$$F_2 = \sqrt{\frac{1+4J^2}{1+(2I-1)^2}}\,\frac{1+\alpha_I\frac{\epsilon_1}{\epsilon_0}(\beta_J)}{1+\beta_J\frac{\epsilon_1}{\epsilon_0}(\beta_J)}$$

$$F_3 = \sqrt{\frac{1+4J^2}{1+4I^2}}\,\frac{1-\beta_I\frac{\epsilon_1}{\epsilon_0}(\beta_J)}{1+\beta_J\frac{\epsilon_1}{\epsilon_0}(\beta_J)}$$

$$F_4 = \sqrt{\frac{1+(2J-1)^2}{1+4I^2}}\,\frac{1-\beta_I\frac{\epsilon_1}{\epsilon_0}(-\alpha_J)}{1-\alpha_J\frac{\epsilon_1}{\epsilon_0}(-\alpha_J)} \quad (21)$$

where

$$\frac{\epsilon_1}{\epsilon_0}(\eta) = \frac{i}{k_0}\left[\frac{h(ik_0,\eta)+h(-ik_0,\eta)}{h(ik_0,\eta)-h(-ik_0,\eta)}\right]$$

and

$$i = \sqrt{-1}. \quad (22)$$

Inverting the Operator Equation

The solution of (7) necessitates the inversion of a semi-infinite matrix operator of the form $\lambda I \pm (S_{BB}+S_{BC}H)T$, where $\lambda = 1.0$. One approach is to expand this in a Neumann series, which is permissible if $|\lambda_n| < 1.0$ for all eigenvalues, λ_n. This leads to the kind of series usually associated with multiple reflections between discontinuities, as in a plane wave passing through a dielectric slab. Indeed, Pace [6] bases his work on a multiple reflection approach, then proves convergence by proving that all $|\lambda_n| < 1.0$.

It is inevitable that the matrices in the Neumann series must be truncated. It becomes just as practical to truncate the operator $(S_{BB}+S_{BC}H)T$ directly, at say J-terms. This has the effect of assuming that only the first J-modes have any significant effect beyond the immediate vicinity of the edge of the septum. Indeed, if the septum is quite long, only the lowest mode is present at the trailing edge of the septum. More terms become significant as the septum becomes shorter, or frequency increases toward the cutoff frequency of the small waveguides in the septum region.

It is reasonable to use the mode decay rate as an indicator of how many terms to include in the truncated matrix.

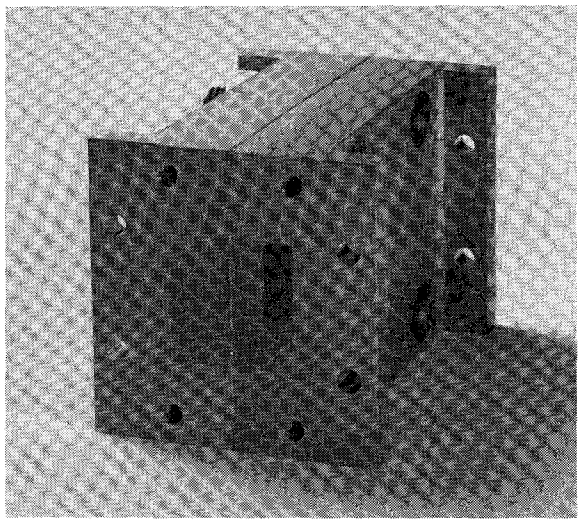

Fig. 4. A septum in a single mount.

This approach was used, with the matrix order J being chosen when $\exp(-\beta_J L)=0.5\times10^{-6}$, but with J never less than two. This rule of thumb proved to be quite practical, since increasing the size of the matrix affected only the fifth significant decimal place of the reflection and transmission coefficient.

It would appear that truncating the matrix would yield inexact solutions. This is not precisely true, because (barring computer round-off errors) a solution is obtainable to any desired degree of accuracy by successively increasing the size of the truncated matrix and taking the limit of the sequence generated.

Single Septum Results

a) *TE_{10} Incident Mode:* For experimental work at X-band, a 0.900 inch (2.286 cm) square waveguide was chosen, with septums made from 0.010 inch (0.0254 cm) copper stock, in lengths ranging from $\frac{1}{8}$ inch to 1 inch in $\frac{1}{8}$ inch (0.3175 cm) increments. A simple split waveguide was used as a septum holder, as shown in Fig. 4. The reflection and transmission coefficients were verified by measuring the argument of S_{11}, and the absolute value of S_{12}, since: 1) $|S_{11}|^2+|S_{12}|^2=1.0$ and 2) Arg S_{11}=Arg $S_{12}\pm90°$ for all symmetrical structures.

Figure 5 shows the measured and calculated insertion loss for several frequencies. The curves marked "thin septum" were computed from the equations given and do not agree with the measured data. This disagreement was traced to the finite thickness of the septum, which altered the values of $\{\gamma_{B_n}\}$ used in the T-matrix of (5). The curves marked "thick septum" were computed by modifying the T-matrix to allow for the septum thickness, but still assuming an infinitely thin septum for determining the elements of the scattering matrices.

A further small deviation was noted for the shorter septums. This was a secondary effect and was traced to the septum edges, which were blunt. Three septums were tapered at a 5° angle, yielding insertion losses that were almost exactly as calculated.

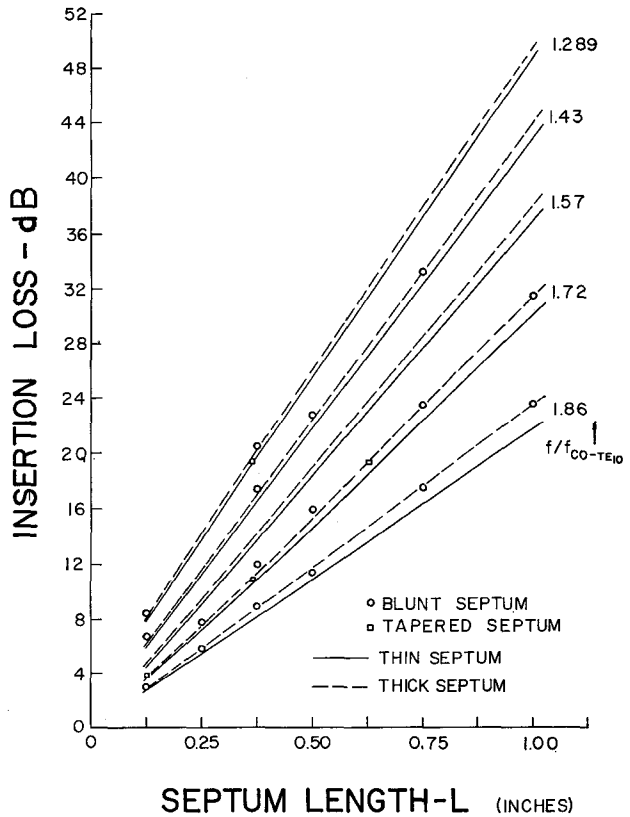

Fig. 5. Single septum insertion loss for the TE_{10} mode.

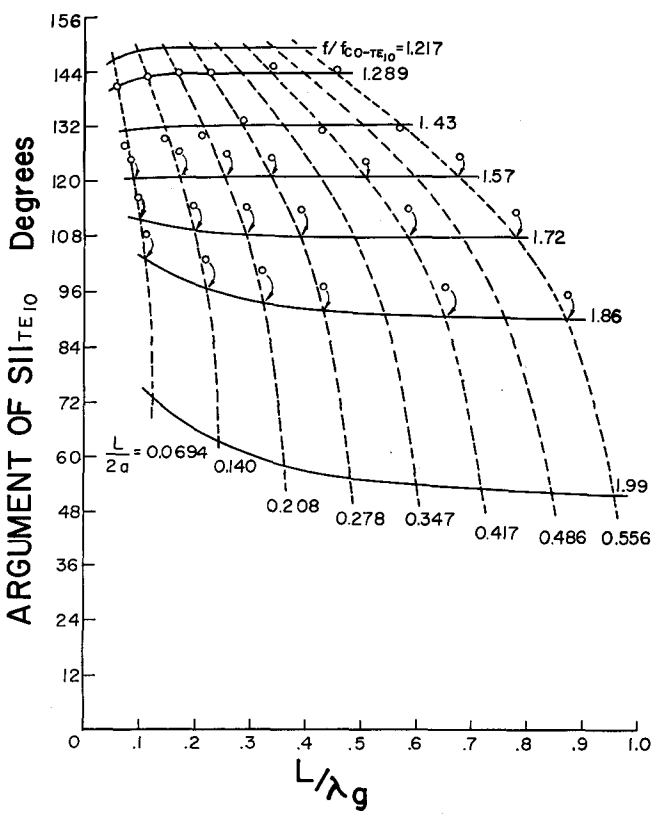

Fig. 6. Argument of the reflection coefficient for a TE_{10} incident mode, for a single septum with a finite thickness.

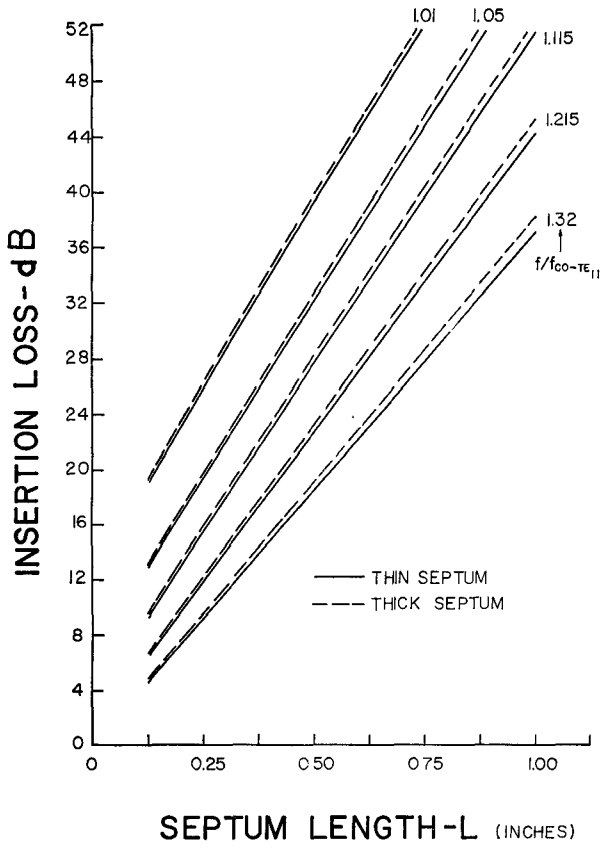

Fig. 7. Single septum insertion loss for the TE_{11} incident mode.

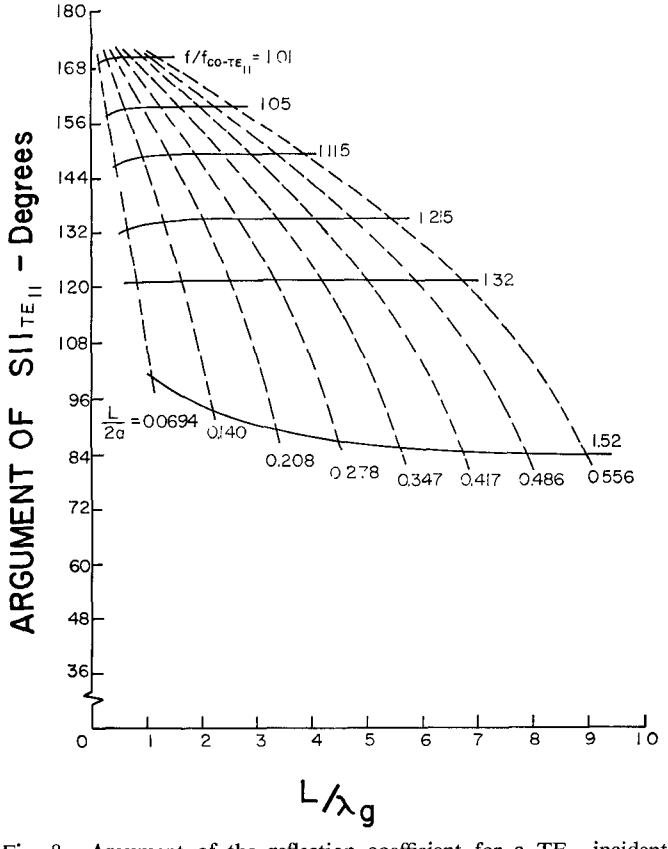

Fig. 8. Argument of the reflection coefficient for a TE_{11} incident mode, for a single septum with a finite thickness.

Figure 6 shows the computed and measured values of Arg S at the same frequencies as previously mentioned.[1] There is a fairly good agreement, with almost all of the discrepancies attributable to the blunt septum edge.

b) *TE_{11} Incident Mode:* The calculated results for the insertion loss and the argument of the reflection coefficient for the TE_{11} mode are presented in Figs. 7 and 8.

c) *TM_{11} Incident Mode:* Figures 9 and 10 show the same data for the TM_{11} mode, but presented in slightly different form. Note that for a constant frequency, increasing the septum length always increases the insertion loss. However, for very short septums of fixed length, increasing the frequency does not always reduce the insertion loss.

The frequency range of interest is above the cutoff frequency f_{co}, α_1 of the main waveguide, and below that of the smaller guides in the septum region f_{co}, β_1. Near f_{co}, α_1, the insertion loss of the septum is quite high, and approaches infinity. Close examination of the elements in the first column of S_{BA} indicates that they are all proportional to α_1. Thus, as α_1 approaches zero at cutoff, the insertion loss increases. Since S_{BA} is the transmission matrix at the leading edge of the septum, low-frequency attenuation is increased by the field behavior at this edge, as well as the attenuation in the septum region itself.

The increase of insertion loss at the high end of the band is partially due to a similar phenomenon at the trailing edge of the septum. One would expect the insertion loss to decrease as the frequency increases toward the cutoff frequency of the lowest-order mode in the septum region. Offsetting this is the fact that for very small values of β_1, the leading term of $(S_{BA}+S_{AC}S_{CA}S_{AB})$ decreases faster than $\exp(-\beta_1 L)$ increases. This is comparable to less transmission of energy, via this mode, past the trailing edge of the septum. For short septums, several modes in the septum region contribute to the total energy transport. Near midband, the lowest-order mode carries a significant proportion of the total. As frequency increases, this mode becomes less important as more of it is reflected at the trailing edge of the septum. Finally, the second mode becomes the dominant contributor to energy transport. But this mode traverses the septum region as $\exp(-\beta_2 L)$, which is attenuated much more than the first mode. Consequently, the total insertion loss increases again.

Fitted Curves

It is not a simple matter to evaluate the formula for the elements of the various matrices. The equations are quite involved and require considerable computer time. For facility of design, fifth degree polynomials have been fitted to the data computed for several frequencies. Once a design engineer chooses a septum length, (23) can be used to compute S_{11}.

[1] The abscissa of Figs. 6, 8, 9, and 10 is normalized with respect to the guide wavelength λ_g of the corresponding lowest-order TE or TM mode in region A. This normalization was introduced to separate curves which would otherwise cross one another and be difficult to interpret.

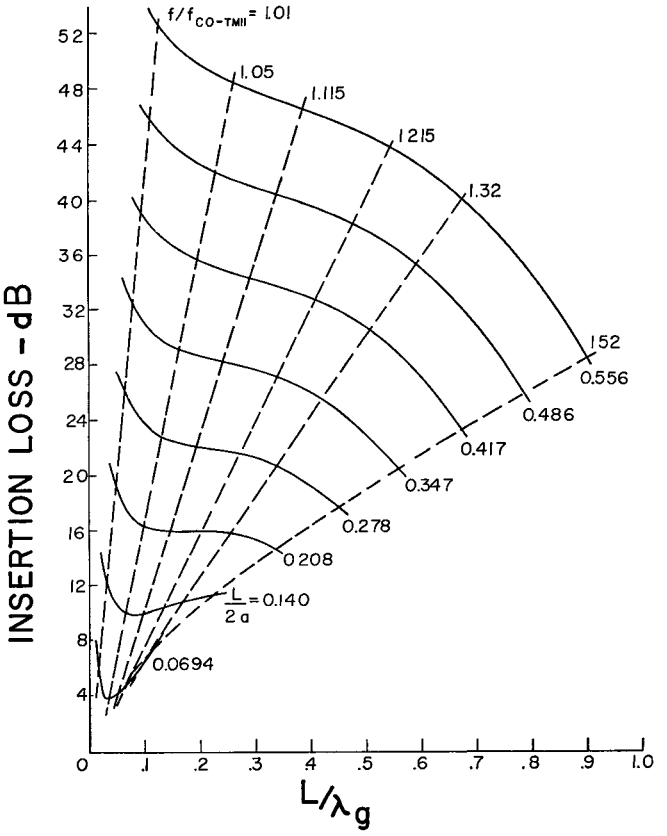

Fig. 9. Single septum insertion loss for the TM_{11} mode.

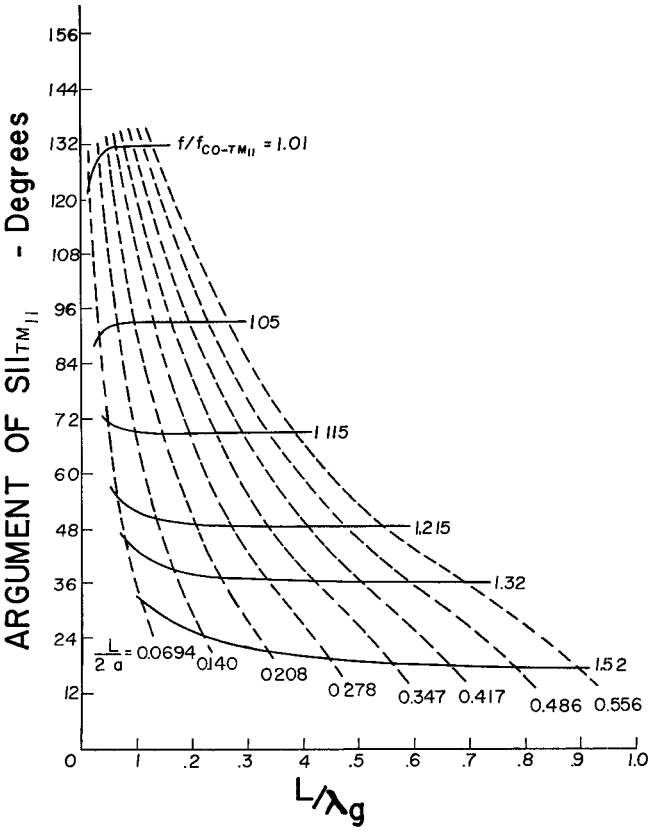

Fig. 10. Argument of the reflection coefficient for a TM_{11} incident mode, for a single septum with a finite thickness.

$$S_{11}(f') = \sum_{N=1}^{6} S11(N) f'^{N-1} \tag{23}$$

where

$$f' = f/f_{co} = k_o/k_{o^{co}}$$

and the $S11(N)$ are presented in Tables I, II, and III for the TE_{10}, TE_{11}, and TM_{11} modes. A similar equation is valid for S_{12}, using the $S12(N)$ in Tables I, II, and III. In the tables, L is the actual length of 0.010 inch thick septums used in 0.900 inch square waveguide. These data can be adapted to other waveguide sizes by applying the scaling factor $L'' = La/0.9$ where "a" is given in inches and by maintaining a septum thickness of $0.011a$.

Frequency has been normalized to the cutoff frequency of the TE_{10} mode for the TE_{10}, TE_{11}, and TM_{11} sets of coefficients. The values of S_{11} and S_{12} computed by using (23) will be quite accurate for frequencies in the range $1.24 \leq f' \leq 1.87$ for the TE_{10} mode. For the TE_{11} and TM_{11} modes, the range of validity is $1.48 \leq f' \leq 1.87$. The range between $f_{co\mathrm{TM}_{11}}$ and $1.05 f_{co\mathrm{TM}_{11}}$ $(1.414 \leq f' < 1.48)$ is not covered by the fitted curves.

Application to Periodic Structures

The basic motivation for this study was to develop a structure capable of inhibiting the TE_{10}, TE_{11}, and TM_{11} modes, while remaining transparent to the TE_{01} mode. Thin septums, far apart, will help, but at certain frequencies depending on spacing, two septums will not help at all, due to the cavity effect. This can be alleviated by random spacing which will sooner or later inhibit any mode at any frequency. Periodic spacing is probably more practical since the structure can be designed to avoid resonant cavities over a given frequency range. This latter approach is discussed below.

With reference to Fig. 11, the transfer scattering matrix for a typical section of the periodic structure is defined as

$$\begin{bmatrix} b_1 \\ a_1 \end{bmatrix} = \begin{bmatrix} T_{11} & T_{14} \\ T_{41} & T_{44} \end{bmatrix} \begin{bmatrix} a_4 \\ b_4 \end{bmatrix} \tag{24}$$

where in this case the subscripts refer to the reference plane. (For several sections in tandem, the combined transfer matrix is simply the product of that of each section.)

By Floquet's theorem, the fields at points one period apart differ by a constant. This constant turns out to be an eigenvalue λ_F of the transfer matrix for a three-part waveguide. The first and third parts are sections of uniform waveguide and the second is a septum section, as shown in Fig. 11.

Let $b_4 = \lambda_F^{-1} a_1$ and $a_4 = \lambda_F^{-1} b_1$. Then (24) leads to

$$\begin{bmatrix} T_{11} - \lambda_F & T_{14} \\ T_{41} & T_{44} - \lambda_F \end{bmatrix} \begin{bmatrix} b_1 \\ a_1 \end{bmatrix} = \begin{bmatrix} 0 \\ 0 \end{bmatrix}. \tag{25}$$

Let $\lambda_F = \exp(p + i\psi)$, so that p is the attenuation of the periodic structure in nepers per period. The two possible eigenvalues λ_{F_1} and λ_{F_2} correspond to Bloch[2] waves traveling

[2] An independent ensemble of eigenfunctions of the uniform waveguide satisfying the discontinuity boundary conditions of the periodic waveguide.

TABLE I

FITTED CURVE COEFFICIENTS FOR THE TE_{10} MODE

N	S11(N) REAL PART	S11(N) IMAG. PART	S12(N) REAL PART	S12(N) IMAG. PART
	SEPTUM LENGTH = .125			
1	-2.255698311457	-9.893780263329	.305770453690	-4.483998961048
2	2.970963623143	26.333153810337	-2.733453175524	10.114433201888
3	-4.057801397111	-28.015854404206	4.457567605160	-7.960692398903
4	3.507641196047	16.013886545442	-2.890890599573	2.881843812332
5	-1.358056746248	-4.836967987896	1.021422331634	-.427334274109
6	.192930322867	.601539084467	-.160034219879	-.003088023244
	SEPTUM LENGTH = .250			
1	-1.847895477002	-8.900739347707	1.936233843491	-1.859846081568
2	1.762736207450	23.923203035337	-8.185847215456	4.155791231616
3	-1.802066795143	-25.857194152868	12.970228941067	-3.176275431807
4	1.062488114710	14.819486889355	-10.060528390276	.902635599253
5	-.174827023513	-4.278157622939	3.952178869099	.123966739852
6	-.001805321372	.474440974484	-.612851521324	-.095037777962
	SEPTUM LENGTH = .375			
1	-1.076847878390	-6.466475229364	3.079847866634	.872236074360
2	-.722904069857	14.519881530322	-11.868016933112	-5.082995451086
3	1.354036799195	-11.304072132079	17.872130789219	9.798278550588
4	-.816705741277	3.516572456102	-13.281177467542	-8.639440796046
5	.281788588808	.109548993671	4.902684613601	3.703740891287
6	-.019680920318	-.199499542726	-.784925073897	-.630203960612
	SEPTUM LENGTH = .500			
1	-2.040244420828	-4.097405419006	2.052877775851	3.127270234168
2	3.336205676629	5.614650988356	-7.470898661604	-12.906463165672
3	-5.370244144041	2.001032248199	10.628298317224	20.790383658095
4	4.699669033936	-6.356685582404	-7.404381211283	-16.458682367920
5	-1.972540461811	3.739864012413	2.516926074395	6.471464420454
6	.348002684927	-.725894840853	-.321160583363	-1.014524483836
	SEPTUM LENGTH = .625			
1	-3.632395648817	-2.874712339277	.263281535419	4.043635909290
2	9.527300770074	1.143991406970	-.507480565979	-15.870871589814
3	-14.929652539158	8.483168536884	-.062626809425	24.617677796140
4	12.036561592940	-11.008963262393	.733963281157	-18.913124901679
5	-4.775183372476	5.387748933420	-.565814474893	7.227039126728
6	.774459058283	-.955092992857	.140491132935	-1.099778767378
	SEPTUM LENGTH = .750			
1	-4.953052609979	-2.487724201082	-1.264183520335	3.994812887751
2	14.565421845218	-.204870158703	5.268398493282	-15.369095412825
3	-22.563970865194	10.335843695265	-8.704879138531	23.442219137723
4	17.784146660053	-12.256689282621	7.142982180277	-17.744237273946
5	-6.926255028689	5.796412461140	-2.922664019053	6.679081615906
6	1.094690483443	-1.006369778988	.481781636200	-1.000196581246
	SEPTUM LENGTH = .875			
1	-5.868448684115	-2.463067844348	-2.245333525786	3.483487909972
2	18.009695491986	-.229954907459	8.891393464436	-13.252415677070
3	-27.713859517643	10.272417887845	-13.997039089682	20.011194863382
4	21.610213505373	-12.132896799685	10.966099003162	-15.004166691396
5	-8.339031991548	5.720907143933	-4.286030941177	5.592210225766
6	1.302132371258	-.990525777026	.671807341270	-.828602365321
	SEPTUM LENGTH = 1.000			
1	-6.421303632743	-2.575098958850	-2.714319136059	2.831355517874
2	20.076262293823	.217471475078	10.556612386826	-10.689704394280
3	-30.783594615820	9.564423368690	-16.323866823477	16.026618286359
4	23.875659452732	-11.577043578763	12.560199795243	-11.932895092650
5	-9.169786360638	5.504004725471	-4.817129966848	4.414912199990
6	1.423241888458	-.956813319437	.738910706088	-.649022019569

TABLE II

FITTED CURVE COEFFICIENTS FOR THE TE_{11} MODE

N	S11(N) REAL PART	S11(N) IMAG. PART	S12(N) REAL PART	S12(N) IMAG. PART
	SEPTUM LENGTH = .125			
1	-1.982226808396	-198.924636758601	-.819737854364	-120.439623037600
2	.552327399611	486.668061476084	-.478084806344	292.934551154176
3	-.995444572473	-470.850905132283	1.261666200207	-281.119257027021
4	1.507986190703	224.932545623232	-.564573263517	132.885846357934
5	-.637345191251	-52.738029441479	.264458856962	-30.728137395744
6	.085241327594	4.815250140726	-.043926176760	2.745526923819
	SEPTUM LENGTH = .250			
1	-1.706100154697	-176.163596411606	-.387144681426	-50.177891547737
2	-.087835888296	432.272566139751	-1.606688823010	122.474831995532
3	1.251610790875	-419.426611018032	4.768733664157	-117.751894516550
4	-1.285477947627	200.519145838006	-4.654474121894	55.381053089331
5	.637674200307	-46.795168441003	2.021029265995	-12.522677611567
6	-.103898568552	4.211755313024	-.317760496773	1.052641118547
	SEPTUM LENGTH = .375			
1	-1.334977151886	-171.980364997398	.252652530562	-22.429522708189
2	-.457310007979	419.884695535976	-2.631151789604	52.764258910483
3	.720263376758	-404.052332242099	5.179852584699	-47.492337892274
4	-.203014658990	190.598000649188	-4.288854417443	19.745496542764
5	-.008866318492	-43.520419126307	1.625789721723	-3.433971788208
6	.026666574577	3.778151144095	-.223425151233	.122865830144
	SEPTUM LENGTH = .500			
1	-1.164002432851	-178.885745652412	.428426906526	-10.014/79877874
2	.534558307078	415.990640981544	-1.477715795359	21.511139090653
3	-2.459148931549	-398.526109153608	1.747792745074	-16.074089042685
4	3.032996926491	186.725389415369	-.888864231626	4.000802774864
5	-1.424728558080	-42.191819999130	.155630801914	.469481556800
6	.255742915332	3.641092094037	.010142910361	-.255654810416
	SEPTUM LENGTH = .625			
1	-1.244138477759	-170.550234264010	.337691554445	-4.373715798326
2	1.952836920434	414.831328995205	.082395563639	7.750596777515
3	-5.684922236961	-396.956014659517	-1.704274989850	-2.948384388844
4	5.949922251746	189.690793998801	2.176472216415	-2.827067964092
5	-2.613864313589	-41.863265810480	-1.074911502923	1.755004840046
6	.438220133404	3.561449613245	.193843521446	-.349031217447
	SEPTUM LENGTH = .750			
1	-1.311066194351	-170.381556787651	.185280034539	-1.825719920205
2	2.890462298066	414.402328948017	1.252844876194	1.960178319035
3	-7.752425387923	-396.855219173023	-3.965853478455	1.908471276037
4	7.788059778456	185.535764851520	4.049775487101	-3.737392922090
5	-3.393084928638	-41.849129012844	-1.786809025554	1.912077852620
6	.550266663593	3.564693378726	.294772632977	-.325187487279
	SEPTUM LENGTH = .875			
1	-1.348952146307	-170.416309062602	.050189501630	-.693847378952
2	3.426161584811	414.618504755526	1.920503330300	-.272/22141668
3	-8.931808450652	-396.963784177787	-5.057349897366	3.221477642883
4	8.833501869332	185.880400456226	4.858741889789	-3.710592821401
5	-3.772004182143	-41.985791486949	-2.064706090264	1.657282886530
6	.613519470031	3.585559630298	.329650232909	-.264687274144
	SEPTUM LENGTH = 1.000 #			
1	-1.404360041804	-170.445869662762	-.043867743054	-.208472073580
2	3.823216188071	414.800100619868	2.176006420286	-.967830523297
3	-9.700481084742	-397.302409928088	-5.294291566307	3.136221902850
4	9.477850580660	186.161636436008	4.930920292633	-3.099928882445
5	-4.022129887096	-42.095316155409	-2.053187988393	1.302977602884
6	.650511859020	3.601937078819	.321955200023	-.201359208167

TABLE III

FITTED CURVE COEFFICIENTS FOR THE TM_{11} MODE

N	S11(N) REAL PART	S11(N) IMAG. PART	S12(N) REAL PART	S12(N) IMAG. PART
	SEPTUM LENGTH = .125			
	A REASONABLE SIZE POLYNOMIAL WILL NOT PROVIDE A GOOD FIT.			
	SEPTUM LENGTH = .250			
1	-340.271780431248	-29.717773586642	-49.368899175649	32.981769057625
2	841.933177455211	22.684455880207	103.429388162112	-18.085186800541
3	-838.542672220501	48.729228828829	-74.106084508111	-56.214139109706
4	420.961636398897	-69.216337707461	17.879823029397	70.498311823466
5	-106.489729957108	30.848073028391	1.479496825845	-29.652424639803
6	10.860093631235	-4.683818303326	-.863129289849	4.328004511659
	SEPTUM LENGTH = .375			
1	-356.768433827346	-74.142378752821	-23.535279841416	-9.013084622478
2	867.469637018803	147.706590462439	45.226666887101	79.343422707388
3	-845.625934156123	-91.531944140733	-26.311757747971	-146.587733692467
4	413.816023785139	9.361027795152	1.064153866971	112.618777172247
5	-101.634575628850	8.847245944605	3.445679008587	-39.549315815689
6	10.025208677361	-2.221623698480	-.788296164592	5.260866539349
	SEPTUM LENGTH = .500			
1	-355.651655986912	-91.454251792456	-6.906368232001	-26.649063937493
2	857.635330308403	198.751439517509	6.591204677528	109.480833871566
3	-827.441341173835	-151.508899951295	7.421114401997	-160.392495868472
4	399.830153718357	44.479538336981	-12.434140884006	110.078513939879
5	-96.717381885491	-1.395050277249	5.748387785797	-36.196731162581
6	9.370312697239	-1.032721798408	-.887701633080	4.614452077623
	SEPTUM LENGTH = .625			
1	-352.433962121904	-99.062994158884	1.148864296989	-30.156323751107
2	845.859578196541	221.999899657566	-11.646522250266	108.117828216563
3	-811.214029617258	-179.692200038334	22.741888575437	-147.044755175193
4	389.092568735359	61.423731333979	-18.148378404352	96.389564818382
5	-93.268492871866	-6.444630890387	6.564524782485	-30.733772909734
6	8.937521234664	-.436524927316	-.894770266131	3.832730230320
	SEPTUM LENGTH = .750			
1	-349.913294634650	-102.616005620438	4.464356926528	-2.202185354446
2	837.421448188251	233.011427984092	-18.441305713538	8.267428096602
3	-800.227251141041	-193.185787971015	27.440805128262	-11.048340805464
4	382.098390059545	69.597479525255	-19.149189553281	6.871673916131
5	-91.083856909826	-8.891567630926	6.397152463441	-2.025725063460
6	8.669120371456	-.147078798831	-.827589035729	.226881034149
	SEPTUM LENGTH = .875			
1	-348.307061473504	-104.175861915246	5.407284371551	-1.240103373644
2	832.180664924089	237.852719480866	-19.583723539977	3.996968955465
3	-793.528515227226	-199.068994418485	26.802981360505	-4.698038844599
4	377.893285065692	73.140540923213	-17.767579866158	2.540698083879
5	-89.784979756223	-9.944295543158	5.727896330876	-.622018103627
6	8.511020810197	-.023708052062	-.721943411241	.051256182149
	SEPTUM LENGTH = 1.000			
1	-347.351911169607	-104.760452563459	5.231104430336	-.666741076657
2	829.103742876031	239.579569998750	-17.919466451239	1.727084558306
3	-789.634782556531	-201.129856470470	23.773156499973	-1.514870732082
4	375.469023125879	74.339161714051	-15.366826131157	.454086071113
5	-89.041436604165	-10.287430640219	4.861265547848	-.032694074421
6	8.421081923224	.014883830245	-.603755667996	-.028119287490

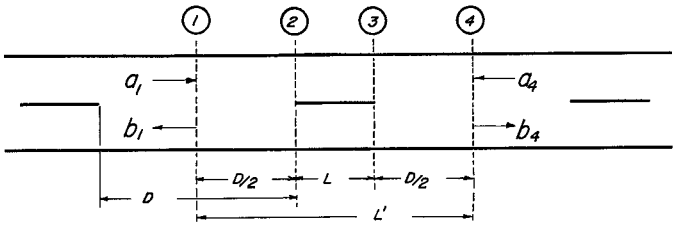

Fig. 11. Transmission system, with septums at periodic intervals.

in the + or $-z$ directions. In the stopbands $\psi=0$ and $p_1=-p_2$. In view of the definition of λ_F, the correct choice of λ_{F_i} for a wave traveling away from a source, in the positive z direction, is for $p>0$, or $|\lambda_{F_i}|>1.0$.

In the passbands, $p=0$, and the correct eigenvalue is chosen in a different way. Note that the ratio of the components of the eigenvectors is $b_1/a_1=\Gamma$, the reflection coefficient seen by a uniform waveguide looking into a periodic waveguide. The correct λ_{F_i} is the one for which $|\Gamma|<1.0$.

Using well-known relations [11] between the scattering matrix and the scattering transfer matrix, the following can be derived:

$$\lambda_{F\pm} = B \pm \sqrt{B^2-1} \tag{26}$$

where $B=\mathrm{Re}[\exp(\alpha_1 D)/S_{12}]$, D is the inter-septum spacing, and S_{12} is for the septum section alone. In the stopbands:

$$\text{Attenuation per section} = 20\log_{10}|\lambda_{F+}|$$
$$|\Gamma| = 1.0 \tag{27}$$

In the passbands:

$$\Gamma = \frac{\exp(\alpha_1 D) - \lambda_{F\pm} S_{12}}{S_{11}} \tag{28}$$

where $\lambda_{F\pm}$ is chosen to make $|\Gamma|<1.0$, the reference plane is midway between septums, and S_{11} and S_{12} are for the septum section alone, as in the first part of this paper.

It has been assumed that all structures are lossless. Small discontinuities are analogous to ideal transformers which connect a main transmission line (TE_{01} mode) to undesired transmission lines (TE_{10}, TE_{11}, and TM_{11} modes). When these latter modes are operating in a stopband, the transformers see an infinite VSWR and no energy is coupled from the main line. Instead, the secondary sees a reactive load with fields decaying at a rate of "p" nepers per period. It follows that the reactive fields generated by each discontinuity are insignificant more than two sections away when the structure is designed for "p" in excess of 10 dB/period.

The design engineer must select an operating frequency and estimate how much isolation is required by the accuracy of his manufacturing process. From this, a septum length is selected. This is aided by noting from (26) that the isolation per period will vary from 0 dB to slightly less than 6 dB in excess of the insertion loss of an isolated septum. Using (23) and Tables I, II, and III, a simple computer routine can be written to enable the selection of the septum spacing. Since α_1 is different for the TE_{10} and the TE_{11} and TM_{11} modes, a compromise spacing may have to be used to inhibit all three modes equally well. Even so, the spacing is not unique, but is determined as a trade-off between bandwidth and attenuation. Wide septum spacing minimizes attenuation and narrow spacing maximizes the width of the stopband.

The contour chart of Fig. 12 is quite useful as a design aid. Ten decibel contour lines are shown for the TE_{10}, TE_{11}, and TM_{11} modes. The closely spaced pairs of curves border bandpass regions for which the modes are attenuated less than 10 dB/period. The diamond shaped areas represent acceptable ranges of spacings and frequency for which all three modes are attenuated more than 10 dB/period. The latter are designated as suppression areas.

The stop bandwidth for a particular septum spacing is the horizontal width of the suppression areas, illustrated by the arrows in the upper right corner.

The design problem simply consists of projecting upward from the desired operating frequency to the largest spacing for which the suppression area is centered and the bandwidth is acceptable.

Figure 12 was generated for use at X-band frequencies and is based on a septum length of 0.500 inch ($0.555a$) in a 0.900 inch (2.286 cm) square waveguide. The region indicated by the lower set of arrows represents a 300 MHz bandwidth centered at 11.38 GHz, with a spacing of 4.45 inches (11.3 cm). The attenuation is 67 percent of that of a conventional waveguide.

When the septum length is varied, the sizes of the suppression areas vary, but the general shape of the curves does not change. For shorter septums, the suppression areas decrease. This is illustrated by the five areas in the lower center which correspond to a septum length of $0.277a$. For longer septums, the suppression areas expand until their borders almost coalesce for lengths greater than the waveguide width.

The peak attenuation per period, in the suppression regions is much less for shorter septums. For $L/a=1.11$, this can be as high as 44 dB/period; for $L/a=0.555$ it falls to 25 dB and for $L/a=0.277$ it falls to 15 dB. As a consequence, septums for which L/a exceed 0.55 are preferable because tuning adjustments are not essential to good performance.

The shaded area in Fig. 12 represents the range between cutoff of the TE_{11} and TM_{11} modes and the lower limit of usefulness of the fitted curves obtained by using (23). It is recommended that this region be avoided.

Related Problems

The analysis presented in this paper may be adapted to other symmetrical waveguide structures. The same basic approach may be used, but with a new T-matrix suitable for the region between the input part and the center of the structure. It would be necessary to show that incident TE modes do not induce TM modes, or the converse, or else to produce a new proof that there are no eigenvalues of the

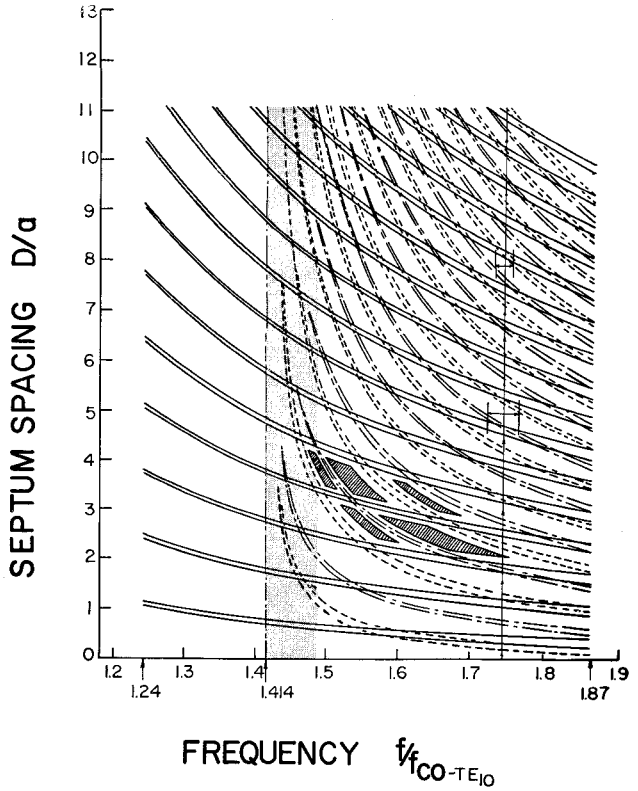

Fig. 12. Decibel contour chart for the TE_{10} mode (———), TE_{11} mode (— — —), and the TM_{11} mode (– – – –).

resulting Fredholm matrix equations that are equal to one.

Only the problem of a square waveguide with a single centered septum has been considered. An interesting problem is posed when the septum is moved off-center so that b/a is no longer 0.5. The second and third line of (3) represent a doubly infinite countable set of equations. They can be reduced to one set by intermixing the equations from each set. In this context, the convergence of the solutions depends on the ratio of equations used from each set. Mittra [12] has shown that for the semi-infinite septum, the correct ratio is b/c, the ratio of the apertures. This suggests that this is the ratio to be used for the finite length septum but it would be an interesting problem to prove this.

Another logical step would be to consider a tall waveguide with P parallel septums. Such a configuration would increase (3) from three semi-infinite sets of equations to P plus two sets. Igarashi [13] has considered the problem of the fields scattered from uniformly spaced semi-infinite septums. His Wiener-Hopf analysis should at least allow one to obtain the coefficients of the various scattering matrices. The principal question would be the method of truncating or intermixing the sets of equations to obtain the correct solution.

Conclusions

The analysis presented in this paper was motivated by a desire to produce a structure capable of inhibiting three of four possible propagating modes by using periodically spaced septums. A new approach to solving the isolated-septum problem has been presented, with fitted curve coefficients tabulated for use over the frequency range of interest. Using these coefficients and/or Fig. 12, it is a relatively simple matter to obtain the parameters of the desired structure.

The TE_{10} mode analysis is not limited to the square waveguide problem, but is also applicable to rectangular waveguides containing centered H-plane septums of arbitrary length.

Acknowledgment

The author would like to express thanks and great appreciation for the gracious, encouraging support of Prof. W. L. Emery, his thesis advisor, and to thank Prof. J. D. Dyson for his helpful constructive suggestions.

References

[1] J. W. E. Griemsmann, "Oversized waveguides," *Microwaves*, pp. 20–31, December 3, 1963.
[2] J. S. Butterworth, A. L. Cullen, and P. N. Robson, "Overmoded rectangular waveguides for high power transmission," *Proc. IEE (London)*, vol. 110, pp. 848–858, May 1963.
[3] M. J. King and J. C. Wiltse, "Very highly overmoded waveguides," *Proc. IEEE (Correspondence)*, vol. 52, pp. 198–199, February 1964.
[4] R. Valenzuela, "Millimeter transmission by oversized and shielded-beam waveguide," *IEEE Trans. on Microwave Theory and Techniques (Correspondence)*, vol. MTT-11, pp. 429–430, September 1963.
[5] C. Ren, "Network representation for lossless symmetrical discontinuities in a multimode waveguide," *IEEE Trans. on Microwave Theory and Techniques*, vol. MTT-14, pp. 81–85, February 1966.
[6] J. R. Pace, "The generalized scattering matrix analysis of waveguide discontinuity problems," Antenna Lab., University of Ill., Urbana, Tech. Rept. 1, Contract AF 19(628)-3819, April 1964.
[7] R. Mittra and J. R. Pace, "A new technique for solving a class of boundary value problems," Antenna Lab., University of Ill., Urbana, Tech. Rept. 72, September 1963.
[8] ——, "Generalized scattering matrix analysis of waveguide discontinuity problems," *Proc. Symp. of Quasi-Optics*, Microwave Research Institute Symposia Series 14. Brooklyn, N. Y.: Polytechnic Press, June 1964, pp. 177–198.
[9] R. A. Hurd and H. Gruenberg, "H-plane bifurcation of rectangular waveguides," *Canad. J. Phys.*, vol. 32, pp. 694–701, November 1954.
[10] D. S. Jones, *The Theory of Electromagnetism*. New York: Macmillan, 1964, pp. 566–569.
[11] M. Sucher and J. Fox, *Handbook on Microwave Measurements*. Brooklyn, N. Y.: Polytechnic Press, 1963, pp. 235–240.
[12] R. Mittra, "Relative convergence of the solution of a doubly infinite set of equations," *J. Res. NBS*, vol. 670, no. 2, pp. 245–254, March–April 1963.
[13] A. Igarashi, "Simultaneous Wiener-Hopf equations and their applications to diffraction problems in electromagnetic theory," *J. Phys. Soc. Japan*, vol. 19, pp. 1213–1221, July 1964.